RESEARCH ARTICLE

A Novel Circularly Polarised Butterfly RF Coil Concept for MRI

SUK-MIN HONG[1], **CHANG-HOON CHOI**[1], **N. JON SHAH**[1,2,3,4],
AND JÖRG FELDER[1,5], **(Senior Member, IEEE)**

[1]Institute of Neuroscience and Medicine 4, INM-4, Forschungszentrum Jülich, 52428 Jülich, Germany
[2]Institute of Neuroscience and Medicine 11, INM-11, JARA, Forschungszentrum Jülich, 52428 Jülich, Germany
[3]JARA-BRAIN-Translational Medicine, 52056 Aachen, Germany
[4]Department of Neurology, RWTH Aachen University, 52056 Aachen, Germany
[5]RWTH Aachen University, 52056 Aachen, Germany

Corresponding author: Suk-Min Hong (s.hong@fz-juelich.de)

ABSTRACT Magnetic resonance imaging (MRI) is an invaluable tool for the diagnosis and study of brain function. Central to the MRI system, the radio frequency (RF) coil plays a dual role: stimulating spins and receiving the MR signal, enabling the generation of detailed images from inside the body. Compared to using linear polarised (LP) methods, the efficiency of the RF coil can be improved by leveraging circular polarised (CP) driving methods, which operate with at least two elements and 90° phase input difference. Coil efficiency can also be improved with the use of a multi-channel phased array receive-only coils, as they provide higher SNR compared to volume coils. Generally, all elements of phased array coils operate in LP mode. However, if the LP elements are replaced by dimension-matched CP elements, the SNR of the phased array coil can be further increased. This study introduces a novel single-channel butterfly coil uniquely capable of operating in CP mode. This is achieved by operating the CP element with asymmetrical tuning and a split resonance peak. The performance of the single-channel CP butterfly coil was evaluated in simulations and MR measurements, and the results were compared to those from single-channel LP coils. The results show that the single-channel CP butterfly coil is a good solution for increasing SNR in phased array receive-only coils.

INDEX TERMS MRI, RF coil, butterfly coil, circularly polarised.

I. INTRODUCTION

The RF coil is an integral part of all MRI systems and serves to stimulate the spin and receive echo signals to enable the production of detailed anatomical images with excellent soft tissue contrast and, when employed in fMRI, information relating to brain function [1], [2], [3]. The performance of the RF coil can be evaluated in terms of transmit efficiency and receiver sensitivity by evaluating the B_1^+ and B_1^- field distribution [4], [5]. The B_1^+ and B_1^- fields are calculated by combining the B_x and B_y fields generated by the coil. B_1^+ and B_1^- fields describe the rotating magnetic field in the xy-plane, and the rotating directions of B_1^+ and B_1^- are counter-clockwise and clockwise, respectively [4], [5]. The

The associate editor coordinating the review of this manuscript and approving it for publication was Sudhakar Radhakrishnan.

B_1^+ field contributes to the transmission of excited spins, and the B_1^- field contributes to the receiver sensitivity.

RF coils are typically categorised into two types: volume coils and surface coils. While volume coils provide very uniform field distribution inside the coil, surface coils provide much higher sensitivity, but only in close proximity to the coil. To overcome these limitations, phased array receive-only coils, consisting of multiple small loop coils (or surface coils) can be used to increase SNR and imaging coverage [6], [7]. The phased array receive-only coil operates in linearly polarised (LP) mode, which generates both B_1^+ and B_1^- fields with identical magnitude but mirrored in the left and right directions, providing much higher SNR than that of a volume coil.

In the early stages of MRI development, circularly polarised (CP) exaction with a volume (birdcage) coil was

explored. The CP mode excitation was considered due to its advantages, provided a gain of square root 2 in the transmission efficiency and low SAR expose [8], [9]. The CP mode birdcage coil is constructed using a two-port feed with a 90° phase input difference. Its efficiency stems from the cancellation of B_1^- the field, allowing the energy to be exclusively used for generating the B_1^+ field.

In contrast, a phased array receive-only coil consists of LP mode elements, where each element generates both B_1^+ and B_1^- fields, and the B_1^+ field does not contribute to the receiver sensitivity. Replacing LP mode elements with CP elements of the same geometrical dimension can significantly enhance the overall receiver sensitivity.

Circular polarisation using surface coils can also be achieved by employing two loops with a 90° phase input difference or a combination of loop and butterfly (or figure-of-eight : FO8) coils [10], [11]. However, the adoption of CP coils requires a minimum of two elements, potentially doubling the total number of channels and reaching the system's limits. Furthermore, the increased number of channels can also potentially increase the coupling between the channels.

A butterfly coil is a surface coil with two single loop elements that resemble the wings of a butterfly. The B_1 field is generated perpendicularly to the plane of the coil and can often be combined with another loop coil in order to generate a quadrature excitation or double-tuned coil assembly [11], [12]. A modified design of a butterfly coil was introduced in the application of a dual-tuned coil at proton/13-carbon frequencies [13]. This design comprises two loops and functions in both common and differential modes [13]. In the differential mode, the feed is positioned at the centre line between the left and right loops, while the feed for the common mode is located on the outer conductor. The current from the common mode of the modified butterfly coil is split into the left and right loops before being recombined for the feed.

In this study, we present a novel design concept for a single-channel CP butterfly coil. For operation in CP mode, the left and right loops of the butterfly coil were tuned with asymmetrical capacitance values. The tuning and performance of the CP butterfly coil were evaluated by simulation and measurements in comparison with the conventional loop coil.

II. METHODS
Simulation

To evaluate the tuning and performance of the proposed CP butterfly coil design, finite integration technique (FIT) simulations were conducted using CST Studio Suite (Dassualt Systems, Vélizy-Villacoublay, France). Fig. 1 shows schematics and simulation models for a rectangular loop coil (10×10 cm^2) and a butterfly coil with identical dimensions. The butterfly coil comprises two loops (left and right loops), with the feed situated at the centre wire. The current in the butterfly coil is split into the left and right loops before being recombined at the feed port.
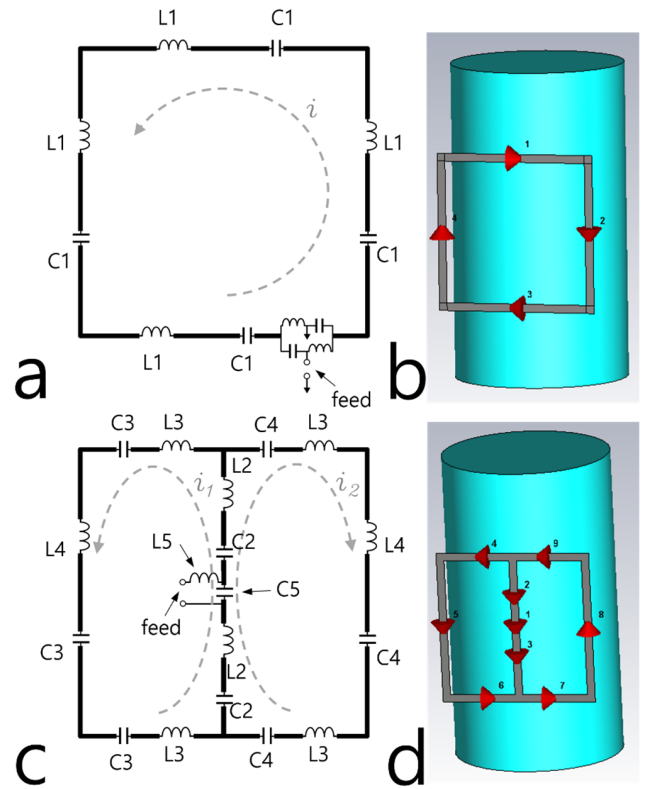

FIGURE 1. Schematics and simulation models of the rectangular loop coil (a, b) and the butterfly coil (c, d).

The conventional coil tuning was achieved based on LC resonance by adjusting inductance (L) and capacitance (C) values to cancel the imaginary part of impedance:

$$Z = RI + j(wL - \frac{1}{wC})I \qquad (1)$$

where Z is impedance, R is resistance, I is current, j is an imaginary number, w is the angular frequency, L is the inductance, and C is the capacitance.

The loop coil (Fig. 1a) was tuned by cancelling the inductance ($4 \times$ L1 = approx. 250 nH for the dimensions given above, with L1 being the inductance created by the wire of one side of the rectangular loop) using $4 \times$ C1, where C1 is given by C1 = $1/(w^2 \times$L1). Following the previously established convention above, the segments of the butterfly were assigned the inductance values L2, L3 and L4, as shown in Fig.1c. The left loop of the butterfly coil (Fig. 1c) was tuned by cancelling inductance ($2 \times$ L2 + $2 \times$ L3 + L4 = approx. 165 nH) using $2 \times$ C2 and $3 \times$ C3. The capacitor value of the right loop was set to $2 \times$ C2 and $3 \times$ C4. In conventional applications, both the left and right loops of a butterfly coil are tuned with identical values, and the current on the left and right loops have identical magnitude but opposite directions (180° phase difference). Thus, the symmetrically tuned butterfly coil operates in LP mode.

In this study, the generation of CP mode using the single-channel butterfly coil involved the intentional

TABLE 1. Capacitance values used to tune the rectangular loop coil, the LC butterfly coil and the CP butterfly coil.

	Capacitance (pF)
C1	4.6
C2 (LP mode/ CP mode)	23 / 25
C3 (LP mode/ CP mode)	6 / 6.1
C4 (LP mode/ CP mode)	6 / 7.8

FIGURE 2. Simulated S-parameters of the LP butterfly coil and the CP butterfly coil.

asymmetrical tuning of the left and right loops of the butterfly coil. Table 1 presents the capacitor values used to tune the loop coil, LP and CP butterfly coil used in the simulation. In the cases where the LP mode tuning was employed for the loop and butterfly coil, the inductance of the coil was almost nullified by capacitors. Conversely, the asymmetrical tuning cancelled out the inductance partially or excessively in both the left and right loops. This resulted in a difference in the phase of the current between the left and right loops and a resonance peak split.

Based on the capacitance values of Table 1, the imaginary impedance difference between the left and right loops of the butterfly coil was approximately 57 Ω. The phase difference between the left and right loops of the butterfly coil due to asymmetrical tuning was evaluated using FIT simulation and compared to that of the LP butterfly coil with conventional, symmetrical tuning. All coils were loaded with a cylindrical phantom (diameter = 11 cm, length = 20 cm, conductivity = 1.0 S/m and permittivity = 80). Ports with an impedance of 50 Ω were positioned at the capacitor and feed locations and were subsequently replaced by capacitors and external ports during co-simulation [14]. To enable efficiency comparisons, the B_1^+ and B_1^- field distributions were normalised using the square root of the accepted power. Additionally, the optimum overlapping distances between the two CP butterfly coils were evaluated in the horizontal and vertical directions. The use of transformer decoupling was also evaluated in the horizontal direction with a 10 mm gap.

Coil construction and MR measurement

The rectangular loop coil (10 × 10 cm^2) and the CP butterfly coil (10 × 10 cm^2) were built and tuned based on the simulation models and results described above. The rectangular loop and CP butterfly coils were built using copper tape (3M, St. Paul, Minnesota, USA). Non-magnetic capacitors (Dalicap Tech.Co.Ltd., China and Voltronics Corp., New Jersey, USA) were used to tune the loop coil and the CP butterfly coil. Both coils were loaded with 2-litre cylindrical phantoms containing 3.75 g NiSO$_4$ × 6H$_2$O + 5 g NaCl per litre. The constructed loop coil and CP butterfly coil were only operated in receive mode and were detuned using a combination of LC trap and PIN diodes [4], [5]. A four-channel CP dipole antenna array was used as the transmission-only coil.

All MR measurements were carried out on a 7 T Terra scanner (Siemens Healthineers, Erlangen, Germany). To evaluate the B_1^- sensitivity of the CP butterfly coil and the loop coil, proton density-weighted gradient echo images were acquired
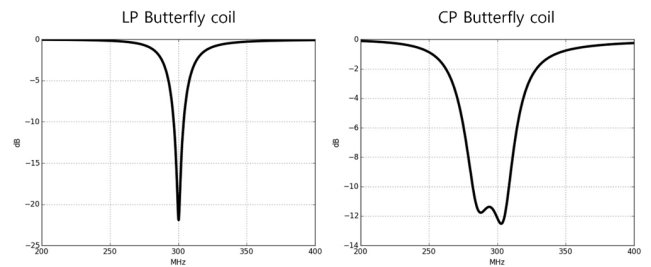
(TR = 3000 ms, TE = 2.55 ms, flip angle = 30° and 60°, pixel bandwidth = 1500 Hz, slice thickness = 1.5 mm, acquisition matrix = 128 × 128, 6/8 partial Fourier, and FoV = 192 × 192 mm^2) in the axial orientation. A sensitivity map was calculated by dividing the SNR map by the flip angle distribution. The flip angle map was acquired using double-angle methods.

III. RESULTS

Fig. 2 shows the simulated S-parameters of the LP and the CP butterfly coils. It can be seen that the LP butterfly coil produces a single resonance peak, whereas the CP butterfly coil produces two split peaks. The frequency difference between the split peaks was 16 MHz, and the reactance difference between the left and right loops was estimated to be around j57 Ω. At 300 MHz, the LP butterfly coil produced −22 dB of S$_{11}$ compared to −12 dB from the CP butterfly coil, which was not optimised.

The simulated isolation between the two loops of the CP-butterfly coils was optimised with a 15 mm and 17 mm overlap in both the vertical and horizontal direction, and the isolation values were 14 dB and 16 dB in the vertical and horizontal direction. The isolation value with a 10 mm gap and transformer decoupling was optimised up to 26 dB.

Fig. 3 shows the simulated current distribution for the loop coil, the LP butterfly coil and the CP butterfly coil at different phases. The left and right loops of the LP butterfly coil were turned on and off during the same phases, whereas the left and right loops of the CP butterfly coil were turned on and off at different phases. The phase difference between the loops was estimated to be around 70°.

Fig. 4 shows simulated B_1^+ and B_1^- efficiency maps generated by the loop coil, the LP butterfly coil, and the CP butterfly coil. The loop and LP butterfly coil provided identical averaged B_1^+ and B_1^- field efficiency values, and the B_1^+ and B_1^- patterns were mirrored in the left and right directions. The loop coil, the LP butterfly coil and the CP butterfly coil provided averaged B_1^+ efficiency values of 0.57 μT, 0.72 μT and 0.43 μT, respectively. The B_1- field values of the loop coil, the LP butterfly coil and the CP butterfly coil were 0.59 μT, 0.73 μT and 0.76 μT, respectively. The CP butterfly coil provided higher averaged B_1^- field efficiency than B_1^+ field efficiency. Fig. 5 shows the profiles of the B_1^- field efficiency
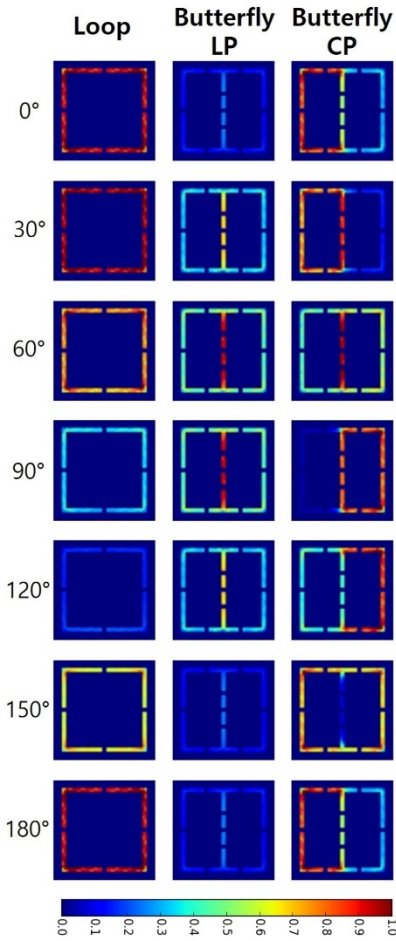
FIGURE 3. Current distribution of the rectangular loop coil (a), LP butterfly coil and CP butterfly coil (b, c) depending on phase. The current patterns were normalised by maximum values of current.
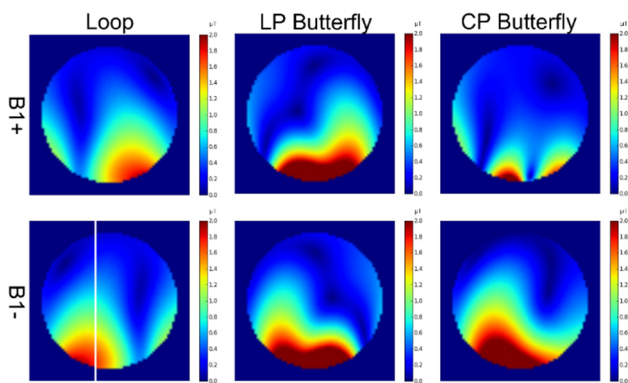

FIGURE 4. Simulated B_1^+ and B_1^- field efficiency generated by the loop coil, the LP butterfly coil and the CP butterfly coil.

generated by all three coils and the ratio between the loop coil and the CP butterfly coil. The LP butterfly coil produced a similar averaged B_1^- efficiency compared to that of the CP butterfly coil, however, the LP butterfly coil provided a more focused field strength near the coil than the CP butterfly coil.
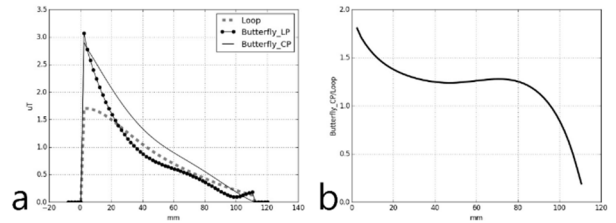

FIGURE 5. B_1^- field efficiency profile (a) generated by the rectangular loop coil, the LP butterfly coil and the CP butterfly coil, and the ratio (b) between the loop coil and the CP butterfly coil.
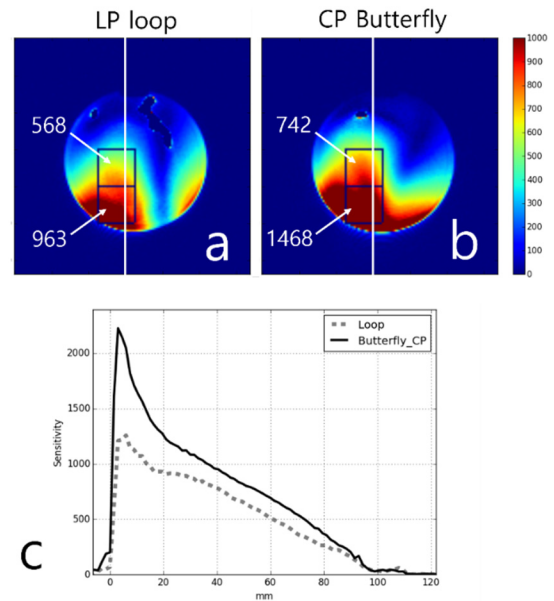

FIGURE 6. Measured receiver sensitivity using the rectangular loop coil (a) and the CP butterfly (b) coil and their profiles(c). The sensitivity provided by each coil was calculated in the selected ROIs.

That being said, the CP butterfly coil demonstrated higher B_1^- efficiency over the 9 cm coverage depth compared to the LP loop coil and LP butterfly coil.

Fig. 6 shows the measured sensitivity maps acquired with the loop coil and the CP butterfly coil. The CP butterfly coil gave higher receiver sensitivity compared to the loop coil in both of the two ROIs and profiles. The higher receiver sensitivity pattern in the ROIs and profiles was in agreement with the simulation results.

IV. DISCUSSIONS
For the LP butterfly coil, capacitors were employed to completely cancel the inductance of both left and right loops, resulting in no imaginary impedance and, thereby, no phased difference. Conversely, in the case of the single channel CP butterfly coil, the deliberate asymmetrical tuning partially or excessively offset the inductance on the left and right loops. This resulted in differences in impedance and phase between the left and right loops, causing the resonance peak of the CP butterfly coil to split.

The S_{11} of the LP butterfly coil and the CP butterfly coil was -22 dB and -12 dB, respectively, whereby the S_{11} of the CP butterfly coil was not optimised while the LP butterfly coil was. This was because the capacitance (C5 : Fig. 1c) needs to be optimised for the matching. As the left and right loops of the CP butterfly coil have different impedances and phases, S_{11} optimisation was difficult with only a single matching capacitor (C5 : Fig. 1c). During transmission, the S_{11} indicates the ratio of the reflected power to the RF power amplifier, while in the receive phase, S_{11} determines the noise figure of the preamplifier. Therefore, the CP butterfly coil is not suitable for the transmission because the less optimised S_{11} would provide more reflected power to the MR system compared to that of the LP mode coils. Conversely, in the receive phase, employing a preamplifier with higher input tolerance could minimise SNR loss. Hence, as the MR measurement results (Fig. 6) agreed with the simulation results (Fig. 4 and 5), it seems that the preamplifier used in the measurement provided enough tolerance.

The polarity of a conventional CP coil is determined by its phase input. However, in the case of the CP butterfly coil, polarity adjustments can be made through tuning rather than manipulating the phase input, as is typically done with conventional CP coils. In both the simulation and the actual RF coil construction, higher capacitor values were used on the right loop. This configuration, as shown in Table 1, resulted in the CP butterfly coil generating a higher B_1^- field distribution compared to the B_1^+ field distribution. Conversely, if higher capacitor values are applied to the left loop, the B_1^+ field efficiency surpasses that of the B_1^- field.

This concept can also be extended to a multi-channel array. To achieve this, the isolation between the loops in the CP butterfly coil could be optimised by adjusting the overlapping distance in both the vertical and horizontal directions. Alternatively, transformer decoupling is also a viable option. In a phased array coil, optimisation is achieved by ensuring isolation between nearest neighbours and applying preamp decoupling to optimise the performance between other channels [7]. However, the use of preamp decoupling on a CP butterfly coil would not be sufficient, as the outer part of the butterfly coil can interact with the outer channel. To optimise isolation between second-nearest or diagonal neighbours, transformer decoupling or self-decoupling methods can be employed [15]. Thus, the use of self-decoupling methods can minimise the current flowing through the outer loop of the CP butterfly coil, resulting in improved channe isolation.

Recent studies of multi-channel phased array coils were evaluated with a high number of channels to cover an identical area. It was found that an increased number of channels leads to a reduction in the size of the coils needed and provides higher SNR near the coil without loss in the deep region. However, the increased number of channels could increase the coupling problem between all channels. In comparison, the CP butterfly coil evaluated in this study in relation to a dimension-matched loop coil achieved improved sensitivity both near the coil and in the deep region without an increase in the number of channels, thereby mitigating potential coupling problems.

V. CONCLUSION

The deliberate asymmetrical tuning of the CP butterfly coil generated a phase delay in the current between left and right loops and implemented a single-channel CP mode element. Although the asymmetrical tuning made the resonance peak of the CP butterfly coil split, and S_{11} was less optimised than in the LC mode coils, the single-channel CP butterfly coil provided higher receiver sensitivity compared to the dimension-matched LP mode loop coil, as evaluated in simulation and MR measurement. The isolation between the CP butterfly loops can be optimised by adjusting the overlapping distance and using transformer decoupling. Therefore, the single-channel CP butterfly coil presents a viable solution for increasing SNR in phased array receive-only coils.

REFERENCES

[1] N. Weiskopf, L. J. Edwards, G. Helms, S. Mohammadi, and E. Kirilina, "Quantitative magnetic resonance imaging of brain anatomy and in vivo histology," *Nature Rev. Phys.*, vol. 3, no. 8, pp. 570–588, Jun. 2021, doi: 10.1038/S42254-021-00326-1.

[2] T. Ai, J. N. Morelli, X. Hu, D. Hao, F. L. Goerner, B. Ager, and V. M. Runge, "A historical overview of magnetic resonance imaging, focusing on technological innovations," *Investigative Radiol.*, vol. 47, no. 12, pp. 725–741, Dec. 2012, doi: 10.1097/RLI.0B013E318272D29F.

[3] M. J. Lowe, "A historical perspective on the evolution of resting-state functional connectivity with MRI," *Magn. Reson. Mater. Phys., Biol. Med.*, vol. 23, nos. 5–6, pp. 279–288, Dec. 2010, doi: 10.1007/S10334-010-0230-Y.

[4] D. I. Hoult, "The principle of reciprocity in signal strength calculations—A mathematical guide," *Concepts Magn. Reson.*, vol. 12, no. 4, pp. 173–187, 2000, doi: 10.1002/1099-0534(2000)12:4<173::AID-CMR1>3.0.CO;2-Q.

[5] C. M. Collins, Q. X. Yang, J. H. Wang, X. Zhang, H. Liu, S. Michaeli, X.-H. Zhu, G. Adriany, J. T. Vaughan, P. Anderson, H. Merkle, K. Ugurbil, M. B. Smith, and W. Chen, "Different excitation and reception distributions with a single-loop transmit-receive surface coil near a head-sized spherical phantom at 300 MHz," *Magn. Reson. Med.*, vol. 47, no. 5, pp. 1026–1028, May 2002, doi: 10.1002/MRM.10153.

[6] G. C. Wiggins, A. Potthast, C. Triantafyllou, C. J. Wiggins, and L. L. Wald, "Eight-channel phased array coil and detunable TEM volume coil for 7 T brain imaging," *Magn. Reson. Med.*, vol. 54, no. 1, pp. 235–240, Jul. 2005, doi: 10.1002/MRM.20547.

[7] P. B. Roemer, W. A. Edelstein, C. E. Hayes, S. P. Souza, and O. M. Mueller, "The NMR phased array," *Magn. Reson. Med.*, vol. 16, no. 2, pp. 192–225, Nov. 1990, doi: 10.1002/MRM.1910160203.

[8] C. M. Collins, S. Li, and M. B. Smith, "SAR and B1 field distributions in a heterogeneous human head model within a birdcage coil," *Magn. Reson. Med.*, vol. 40, no. 6, pp. 847–856, Dec. 1998, doi: 10.1002/MRM.1910400610.

[9] G. H. Glover, C. E. Hayes, N. J. Pelc, W. A. Edelstein, O. M. Mueller, H. R. Hart, C. J. Hardy, M. O'Donnell, and W. D. Barber, "Comparison of linear and circular polarization for magnetic resonance imaging," *J. Magn. Reson.*, vol. 64, no. 2, pp. 255–270, Sep. 1985. [Online]. Available: https://www.sciencedirect.com/science/article/pii/002223648590349X

[10] C.-H. Choi, S.-M. Hong, J. Felder, and N. J. Shah, "The state-of-the-art and emerging design approaches of double-tuned RF coils for X-nuclei, brain MR imaging and spectroscopy: A review," *Magn. Reson. Imag.*, vol. 72, pp. 103–116, Oct. 2020, doi: 10.1016/J.MRI.2020.07.003.

[11] D. W. J. Klomp, "Radio-frequency probe for ^{1}H decoupled ^{31}P MRS of the head and neck region," *Magn. Reson. Imag.*, vol. 19, no. 5, pp. 755–759, Jun. 2001, doi: 10.1016/S0730-725X(01)00390-3.

[12] M. Alfonsetti, A. Sotgiu, and M. Alecci, "Design and testing of a 1.5 Tesla double-tuned (1H/31P) RF surface coil with intrinsic geometric isolation," *Measurement*, vol. 43, no. 9, pp. 1266–1276, Nov. 2010, doi: 10.1016/J.MEASUREMENT.2010.07.003.

[13] P. Cao, X. Zhang, I. Park, C. Najac, S. J. Nelson, S. Ronen, and P. E. Z. Larson, "1H-13C independently tuned radiofrequency surface coil applied for in vivo hyperpolarized MRI," *Magn. Reson. Med.*, vol. 76, no. 5, pp. 1612–1620, Nov. 2016, doi: 10.1002/MRM.26046.

[14] M. Kozlov and R. Turner, "Fast MRI coil analysis based on 3-D electromagnetic and RF circuit co-simulation," *J. Magn. Reson.*, vol. 200, no. 1, pp. 147–152, Sep. 2009, doi: 10.1016/J.JMR.2009.06.005.

[15] X. Yan, J. C. Gore, and W. A. Grissom, "Self-decoupled radiofrequency coils for magnetic resonance imaging," *Nature Commun.*, vol. 9, no. 1, p. 3481, Aug. 2018, doi: 10.1038/S41467-018-05585-8.

CHANG-HOON CHOI received the Ph.D. degree in MRI physics from the University of Aberdeen, Aberdeen, U.K., in 2010. He was with MR Solutions Ltd., Guildford, U.K., until 2014. He is currently an MR Expert. Since 2014, he has been a Senior Scientist with the Forschungszentrum Jüelich, Germany.

N. JON SHAH received the Ph.D. degree from The University of Manchester. He went to Japan, where he worked on the development of methods for MRI and spectroscopy. He was with the University of Cambridge on MR. Then, he moved to Germany with Forschungszentrum Jüelich, where he is currently the Director of the Institute of Neuroscience and Medicine 4 and 11. He is also a Professor of MRI physics with RWTH Aachen and an Adjunct Professor with the Melbourne Biodiversity Institute (MBI), The University of Melbourne.

SUK-MIN HONG received the Ph.D. degree in medical science from Gachon University, South Korea, in 2013. He was with the Neuroscience Research Institute, South Korea, until 2014. He is currently an RF Coil Expert. Since 2014, he has been a Researcher with the Forschungszentrum Jüelich, Germany.

JÖRG FELDER (Senior Member, IEEE) received the Diploma degree in electrical engineering and the Ph.D. degree from RWTH Aachen University, Aachen, Germany, in 1998 and 2004, respectively. From 2004 to 2007, he was an RF Engineer with Bruker BioSpin MRI GmbH, Ettlingen, Germany. Since 2007, he has been the Team Leader of Forschungszentrum Jüelich, Germany.

• • •